Original Article

Institution of MECHANICAL ENGINEERS
Journal of ENGINEERING MANUFACTURE

Proc IMechE Part B:
J Engineering Manufacture
1–11

DOI: 10.1177/0954405420963004
journals.sagepub.com/home/pib
SAGE

Effect of pre-rolling temperature on the interfacial properties and formability of steel-steel bilayer sheet in Single Point Incremental Forming

Malik Hassan[1], Ghulam Hussain[1], Aaqib Ali[1], Muhammad Ilyas[1], Sohail Malik[1], Wasim A Khan[1] and Burak Bal[2]

Abstract

The aim of this research was to investigate the effect of pre-rolling temperature on the interfacial properties in delamination modes 1 and 2; and formability in Single Point Incremental Forming (SPIF) of Steel-Steel (St-St) bilayer sheet prepared by roll bonding process. The roll bonding process was performed at three pre-rolling temperatures, 700°C, 800°C, and 950°C, with a constant thickness reduction ratio of 58%. The bond strength and critical strain energy release rate (CSERR) were measured to characterize the interface of St-St bilayer sheet. T-peel test for mode 1 and tensile shear test for mode 2 were conducted to determine the interfacial properties. The formability of St-St bilayer sheet in SPIF was measured in terms of maximum wall angle. The results showed that the increase in pre-rolling temperature from 700°C to 950°C enhanced the bond strength and CSERR, in both mode 1 and 2. The enhancement in bond strength with an increase in pre-rolling temperature was 149.5% and 203% in mode 1 and 2, respectively. However, the increase in CSERR in mode 1 and 2 was 115% and 367%, respectively. The formability of St-St bilayer sheet also showed an increasing trend with an increase in pre-rolling temperature. Moreover, a consistent relation between formability and interfacial parameters was observed. It was also found that to successively deform the bilayer sheet into the desired shape, it is necessary for the sheet to be heated above the critical temperature during fabrication to facilitate good bonding between two sheets.

Keywords

Pre-rolling temperature, Single Point Incremental Forming, bond strength, critical strain energy release rate, formability

Date received: 9 July 2019; accepted: 23 August 2020

Introduction

Single Point Incremental Forming (SPIF) is an innovative sheet metal forming process. It does not require dedicated tooling and is performed by using computer numerical control (CNC) technology. In comparison to traditional sheet forming processes, SPIF is more flexible with respect to the complexity of shape and tooling.[1,2] In this process, the forming tool moves in increments to produce highly localized plastic deformation.[3,4] Because of the flexibility and adaptability of this process, SPIF can be used in the manufacturing of medical implants and automobile parts, etc.[5–7] For instance, Ambrogio et al.[8] and Oleksik et al.[9] manufactured highly customized ankle support and knee implants, respectively, by using SPIF. Bagudanch et al.[10] exhibited that through SPIF, it is conceivable to develop a highly customized cranial implant by utilizing a biocompatible polymer. Behera et al.[11] manufactured a 3D human face mask by using the SPIF technique which was a novel contribution of the SPIF. Li et al.[12] employed a multipass strategy of SPIF to process the taillight bracket of a car without apparent cracks and wrinkles. It is worth noting that SPIF can be used to manufacture complex and asymmetric parts.[13] SPIF is

[1]Faculty of Mechanical Engineering, Ghulam Ishaq Khan Institute of Engineering Sciences and Technology, Topi, Pakistan
[2]Department of Mechanical Engineering, Abdullah Gül University, Kayseri, Turkey

Corresponding author:
Ghulam Hussain, Faculty of Mechanical Engineering, Ghulam Ishaq Khan Institute of Engineering Sciences and Technology, Topi 23640, Pakistan.
Emails: ghulam.hussain@giki.edu.pk; gh_ghumman@hotmail.com

considered as the most adequate processes for the forming of layered metallic materials (LMMs).

To fabricate LMMs, an effective process in terms of cost and production of a large bonding area is hot roll bonding.[14] Hot roll bonding is also the most commercially used method for the fabrication of steel-clad plates.[15] Zhang et al.[16] presented a bond criterion for hot-rolled laminated metallic composites. In hot roll bonding, at the base metal plate's interface, two regions, bonded and unbonded regions, exist. The bond criterion developed by Zhang et al.[16] depends upon the definition of strain and bond strength thresholds. Strain threshold demonstrated that during rolling, the base metal plates cannot be bonded at the interface until the strain is larger than a threshold strain. Bonding strength threshold manifested that the separation of the bonded interface would not occur until the interface bond strength would become greater than the critical bond strength.

Liu et al.[17] evaluated the tensile and fracture behavior for cladded plates of stainless steel prepared through hot roll bonding. They proposed that with an increase in bonding temperature, the enhancement in interfacial shear strength can be maintained due to sufficient diffusion of alloy elements. Dhib et al.[14] analyzed in depth the dynamics of hot-rolled low-carbon/austenitic stainless steel clads, based primarily on the clad mechanical properties and microstructure behavior. In another study, Dhib et al.[18] evaluated the joining potential of low carbon and austenitic stainless steel from the hot-roll bonding technique. They evaluated the interface and mechanical properties of the clad sheet. The results revealed that good mechanical properties were obtained for clad produced by means of hot roll bonding. Saboktakin et al.[19] investigated metallurgical and mechanical properties of Titanium cladding on Steel prepared by hot roll bonding. They depicted that the thickness and microhardness of interface depend on bonding temperature. Peng et al.[20] studied the effect of rolling temperature on the bond strength of Cu/Al metal clad and found that the peel strength of the clad increases with an increase in roll bonding temperature. Hosseini and Danesh Manesh[21] fabricated Ti/Cu/Ti composites by roll bonding and measured the bond strength of the clad using a peel test. They concluded that bond strength increased significantly because of enhancement in rolling temperature.

The research work published on the SPIF of LMM's is mainly focused on analyzing the formability. Al-Ghamdi and Hussain[22] investigated the formability of the clad sheet of Cu/Steel. They observed that the formability of LMM's, as that of monolithic sheets, increases as the tensile area reduction increases. In another study,[23] they investigated the effects of process parameters on the formability of the Cu-Steel-Cu clad sheet. The results showed that increased tool rotation does not necessarily raise the formability of the clad sheet. The formability increase was realized under specific conditions especially when the tool diameter, step size, and feed rate were small and annealing of the clad sheet was performed at a low temperature. In another study, Al-Ghamdi and Hussain[24] compared the formability of the clad sheet in SPIF and Stamping and reported that SPIF offered 923% greater formability than stamping. Alinaghian et al.[25] studied the effect of tool diameter, rotational speed, and step size on residual stress of Al/Cu clad in SPIF. They measured residual stresses through the hole-drill method. The finite-element analysis was conducted to evaluate the calibration coefficients. The results depicted that tool diameter and step size can affect the residual stress. While the rotational speed of the tool had no effect on the residual stresses.

Gheysarian and Honarpisheh[26] experimentally explored the effect of layer arrangement on thickness distribution, formability, forming force and surface roughness of explosively-welded Al-Cu bimetal sheets. Keeping Al as an inner layer resulted in larger forming force and low formability thereby showing the effect of yield strength of the layer material on these quantities. Honarpisheh et al.[27] performed an experimental work to assess the formability of Al/Cu sheets. The maximum formability occurred employing a large step size, small tool diameter, and tool rotational speed. Ashouri and Shahrajabian[28] investigated Brass-St clad formability and identified that an increase in tool diameter from 10 to 20 mm, resulted in a drop in formability from 69° to 58.5°. Similarly, an increase in the vertical step size and feed rate caused a reduction in the formability. Hassan et al.[29] analyzed the delamination failure of roll bonded St-St bilayer sheet in SPIF. They heated the constituting sheets in a furnace at a constant temperature of 950°C prior and then subjected them to three different rolling reduction ratios of 47%, 58%, and 70%. The formability decreased with increasing the reduction ratio, and further a bulk failure was observed.

The pre-rolling temperature is an important parameter as it is likely to affect the interfacial bonding, fracture toughness, and hence the failure of the layered sheet. Till now, this specific subject has not been addressed in the SPIF literature. Therefore, in order to comprehend the knowledge, there is a need to perform work in this direction. In the present study, bilayer St-St sheet was fabricated through rolling by considering three pre-rolling temperatures, 700°C, 800°C, and 950°C and a constant thickness reduction ratio of 58%. Two monolithic sheets, measured to a combined thickness of 2.85 mm, were subjected to rolling which resulted in a bilayer bonded sheet of 1.2 mm thickness. Later, the T-peel and tensile shear tests were conducted on the bilayer sheets to determine the influence of changing pre-rolling temperature on the interfacial properties, that is, bond strength and critical strain energy release rate (CSERR) in mode 1 and mode 2.

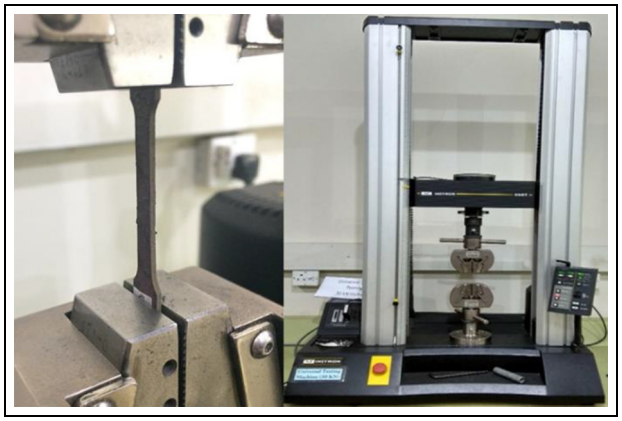

Figure 1. Experimental setup for tensile testing.

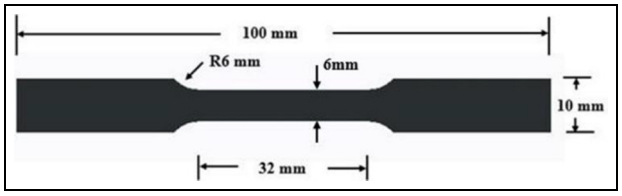

Figure 2. Dimensions of the subsidized tensile sample as per ASTM standard.

Moreover, formability tests were executed on the fabricated sheets in order to identify the role of temperature on their formability in SPIF.

Tensile testing

The material used in this study was deep drawing quality steel EN 10130 Grade DC03. Tensile tests were conducted by Universal Testing Machine (INSTRON-5567) at a crosshead displacement speed of 2 mm/min to investigate the mechanical properties of St-St bilayer sheets at different pre-rolling temperatures. The experimental setup of the tensile test is shown in Figure 1. These tests were performed following ASTM E8M Standard.[30] Figure 2 depicts the dimensions of the tensile test sample.

Interface characterization

The St-St bilayer sheet interface was defined in both modes 1 and 2, in terms of bond strength and CSERR. Three samples were fabricated and tested for every condition that is three pre-rolling temperatures 700°C, 800°C, and 950°C at a constant thickness reduction ratio of 58%.

Mode 1 delamination test

T-peel test was performed to evaluate the bilayer sheet interfacial properties in mode 1. The tests were conducted according to the procedure mentioned in ASTM standard D1876.[31] Tests were performed using 30 kN electro-mechanical controlled Instron machine (INSTRON-5567) at a displacement rate of 2 mm/min. The experimental setup for the T-peel test is shown in Figure 3. The interfacial bond strength of bilayer sheet can be determined by using the relation $\sigma_I = \frac{Average\ peel\ load}{Bond\ width}$.[32] The CSERR can be calculated using equation $G_c = \frac{12P_c^2a^2}{b^2h^3E}$,[33] in which P_c is the crack initiation load, a is the initial crack length determined by the relation $a = \sqrt[3]{\frac{Ebh^3C}{8}}$, E represents Young's modulus, the thickness of a single steel sheet is represented by h, b shows the specimen width and C is the elastic compliance of the test specimen.

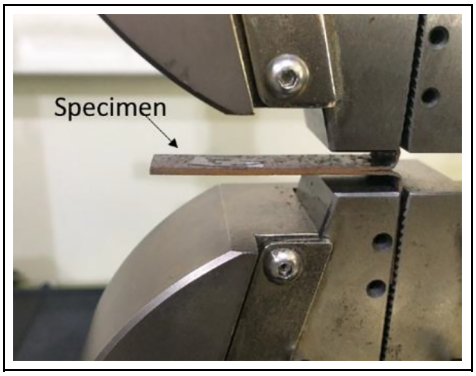

Figure 3. Experimental setup of T-peel test.

Mode 2 delamination test

The interfacial bonding properties of the St-St bilayer sheet under shear load were determined by performing the tensile shear test. The tests were conducted according to the procedure given in ASTM standard D1002.[34] The schematic of the experimental setup for the tensile shear test is shown in Figure 4. Figure 5 depicts the dimension of the tensile shear test sample. For mode 2, the interfacial bond strength can be determined using equation $\sigma_{II} = \frac{P_c}{A_{overlap}}$,[35] in which P_c is load at initiation of crack. The CSERR can be obtained using relation $G_c = \frac{1}{2}T_{max}\left(\delta_{c1} + 2(\delta_{c2} - \delta_{c1}) + \left(\delta_f - \delta_{c2}\right)\right)$,[36] in which, T_{max} is the limiting contact strength, δ_{c1} is the damage initiation displacement, δ_{c2} is the displacement at end of plateau region and the displacement at failure is represented by δ_f as shown in Figure 6.

Experimentation of SPIF

The experiments for SPIF of St-St bilayer sheet were performed on three-axis CNC machine (TRIAC FANUC). The 10 mm diameter high-speed steel hemispherical tip forming tool was used to deform the 100 mm diameter circular blank. The experimental setup for SPIF is shown in Figure 7. The feed rate and step depth were considered to be 1300 mm/min and

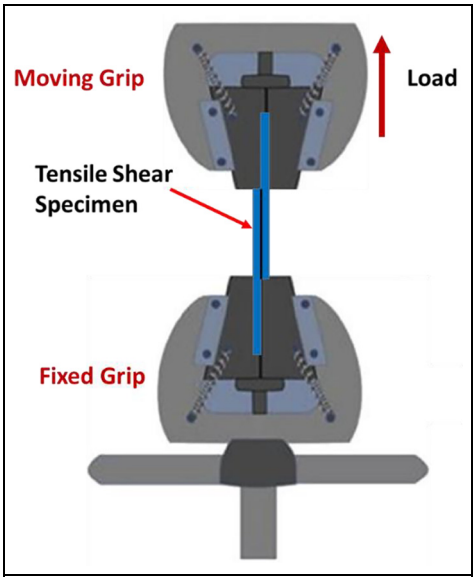

Figure 4. Schematic representation of the tensile shear test.

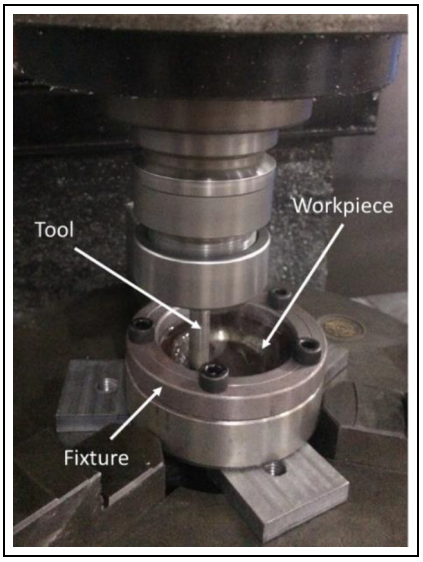

Figure 7. Experimental setup for SPIF.

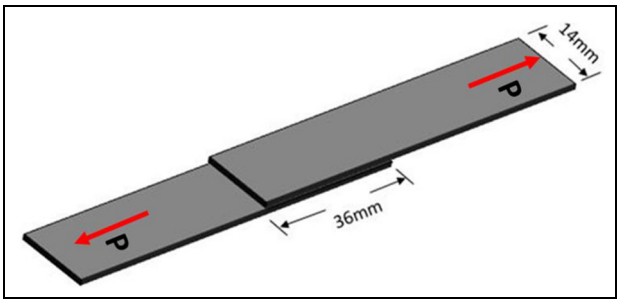

Figure 5. Dimension of the tensile shear test sample.

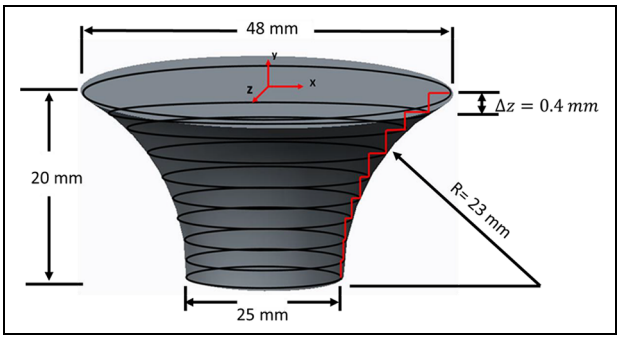

Figure 8. Varying wall angle cone (VWAC) tool trajectory.

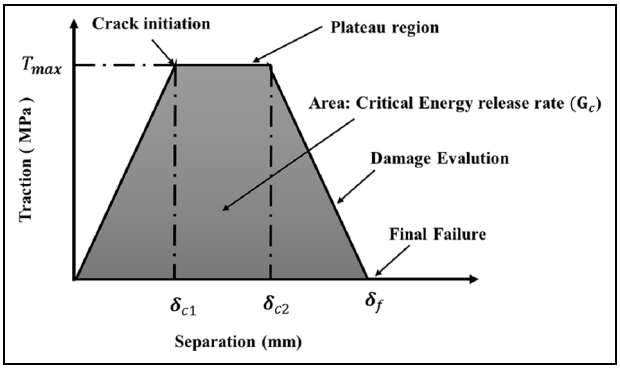

Figure 6. Trapezoidal separation law for mode 2 delamination test.

0.4 mm, respectively, without spindle rotation. Mineral oil was used to reduce friction between tool and workpiece. The deformed shape of the workpiece depends on the toolpath given to tool.[37] The test geometry used was varying wall angle cone (VWAC) with 48 mm major diameter and 25 mm minor diameter as shown in Figure 8. The designed depth was taken as 20 mm and the radius of generatrix was 23 mm. The angle of VWAC geometry was varied from 30° to 90° and the maximum wall angle at which failure occurred was measured using the relation $\psi_{max} = \cos^{-1}\left(\frac{y_1 - h_f}{R}\right)$,[38] in which, y_1 is the designed depth, h_f is the failure depth and R is the radius of generatrix. The maximum wall angle ψ_{max} is the most critical parameter in predicting formability.[39]

Results and discussion

Effect of pre-rolling temperature on yield strength and interfacial properties

The effect of pre-rolling temperature on the yield strength of the St-St bilayer sheet is shown in Figures 9 and 10. It can be seen that yield strength decreases with an increase in pre-rolling temperature from 700°C to 950°C at a constant thickness reduction ratio of 58%. The average yield strengths at three pre-rolling temperatures of 700°C, 800°C, and 950°C were found to be 350±31, 280±15, 250±17 MPa, respectively. It may be attributed to the fact that at high temperature, the

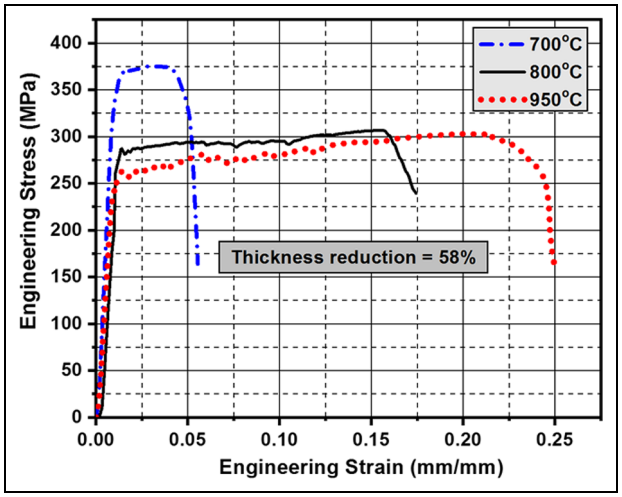

Figure 9. Engineering stress versus engineering strain plot of St-St bilayer sheets joined at various pre-rolling temperatures.

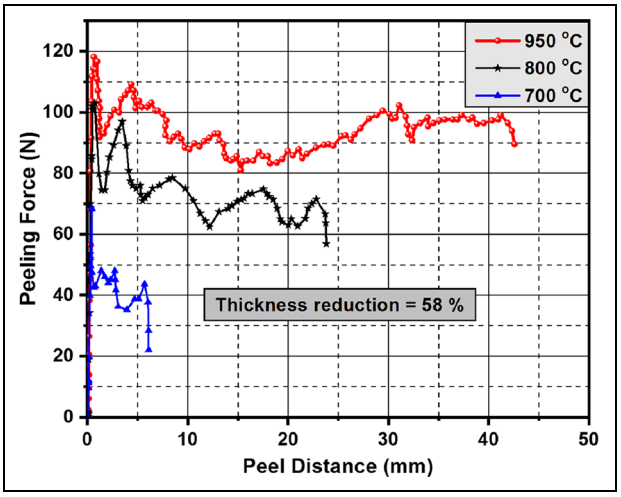

Figure 11. Force-displacement plot for variation in temperature in mode 1.

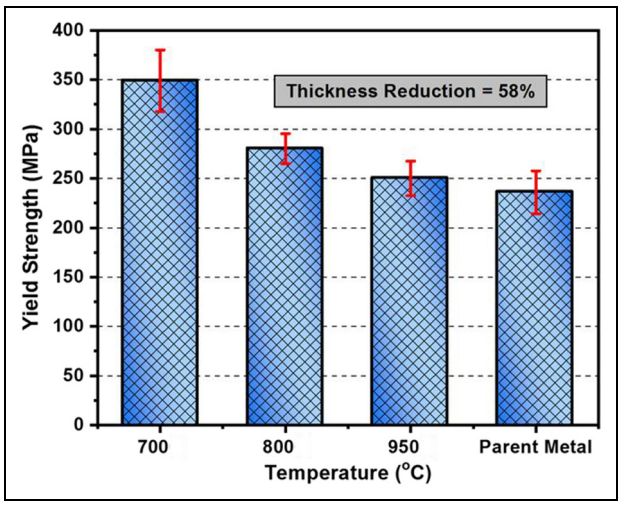

Figure 10. Variation in St-St bilayer sheet yield strength versus pre-rolling temperature.

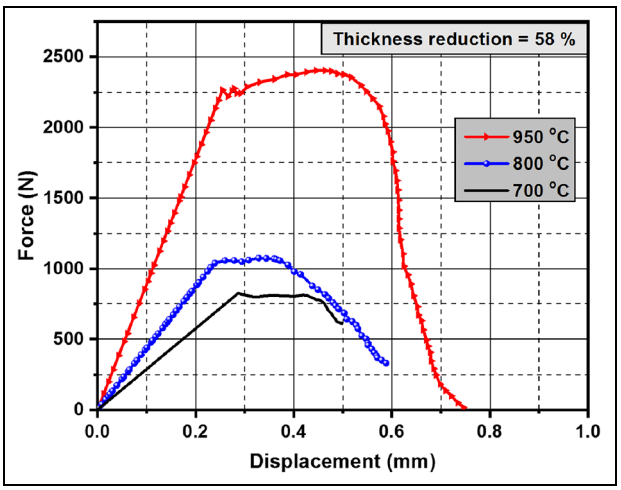

Figure 12. Force-displacement plot for variation in temperature in mode 2.

grains become coarse, while grain refinement occurs at low pre-rolling temperature. At low temperature, the grain size is small as a result high density of grain boundaries occurs which hinders the movement of dislocations, results in enhancement of yield strength.[40,41]

The effect of pre-rolling temperature on the force-displacement plots for the St-St bilayer sheet in mode 1 and 2 are depicted in Figures 11 and 12, respectively. As can be seen from Figures 13 and 14, the bond strength increases with increasing pre-rolling temperature, that is, 700°C, 800°C, and 950°C at a constant thickness reduction of 58% in both modes 1 and 2, respectively. The bond strength in mode 1 increases from $2.1\pm0.65\ ^{N}/_{mm}$ at a pre-rolling temperature of 700°C to $5.24\pm1.7\ ^{N}/_{mm}$ at a pre-rolling temperature of 950°C. This increase in bond strength is about 149.5%. Moreover, bond strength in mode 2 also varies similarly with values ranging from $1.58\ \pm0.08$ MPa at pre-rolling temperature of 700°C to $4.8\ \pm0.007$ MPa at pre-rolling temperature of 950°C. The increase in bond strength with an increase in pre-rolling temperature in mode 2 is 203%. Figure 15 shows that CSERR for mode 1 increases with the increase in pre-rolling temperature with values ranging from $276\pm20.8\ ^{J}/_{m^2}$ at pre-rolling temperature of 700°C to $594\pm44\ ^{J}/_{m^2}$ at pre-rolling temperature of 950°C which is an increase of 115%. The CSERR for mode 2 also depicts the increasing trend with the increase of pre-rolling temperature that is, from $500\pm26\ ^{J}/_{m^2}$ at 700°C to $2335\pm43\ ^{J}/_{m^2}$ at 950°C, an increase of 367% as shown in Figure 16.

The XRD analysis of the peel surface showed that at high temperature, only ferrous oxide (FeO) formed while at low temperature, magnetite (Fe_3O_4), as well as FeO, were formed, as can be seen from Figure 17.

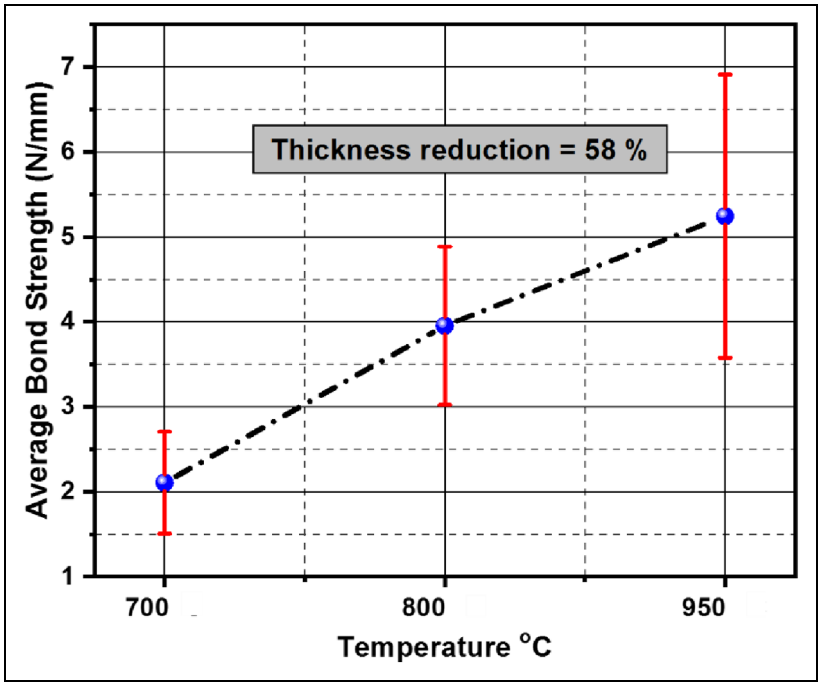

Figure 13. Variation of St-St bilayer sheet average bond strength versus temperature for mode 1.

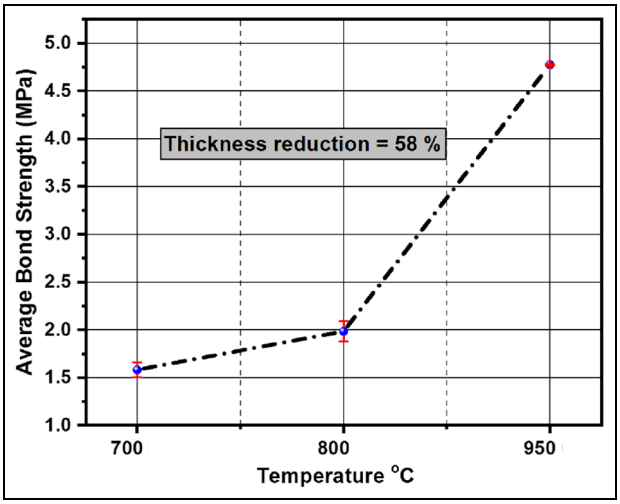

Figure 14. Variation of St-St bilayer sheet average bond strength versus temperature for mode 2.

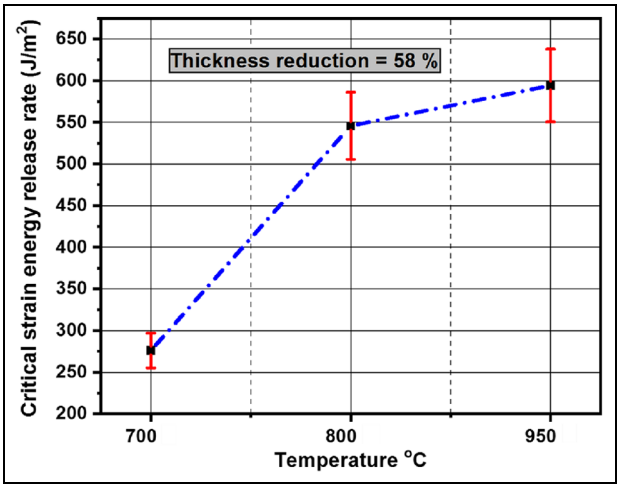

Figure 15. Variation of CSERR versus temperature for mode 1.

Furthermore, the relative intensity of the oxide peaks in comparison to the main Fe peak decreased with an increase in pre-rolling temperature. In comparing the individual intensities of oxides formed, a decreasing trend with increasing pre-rolling temperature was observed along with the change in the type of oxides formed. Also, the Fe peaks at 950°C in comparison to the 700°C shifts to the right highlighting the change in lattice parameters as a result of the annealing process occurring at the high pre-rolling temperature. Since at high temperature, the oxide formation is small, a strong bond between two sheets was observed. While at low temperatures due to the large formation of oxides which act as a barrier to bonding results in low bond strength and CSERR. Yan and Lenard[42] have reported that the temperature affects the oxidation level such that a high temperature reduces the oxidation. This, in turn, raises the interfacial bond strength between the two laminates while rolling. Moreover, increased temperatures promote recovery and recrystallization resulting in the formation of a stronger bond between the metallic sheets.[20] Abbasi and Toroghinejad[43] and Eizadjou et al.[44] showed that as the roll bonding temperature increases, the flow stress of metal decreases. Subsequently, the ductility, formability, and extrusion of virgin metals through cracks increase thereby increasing the surface area available for bonding and

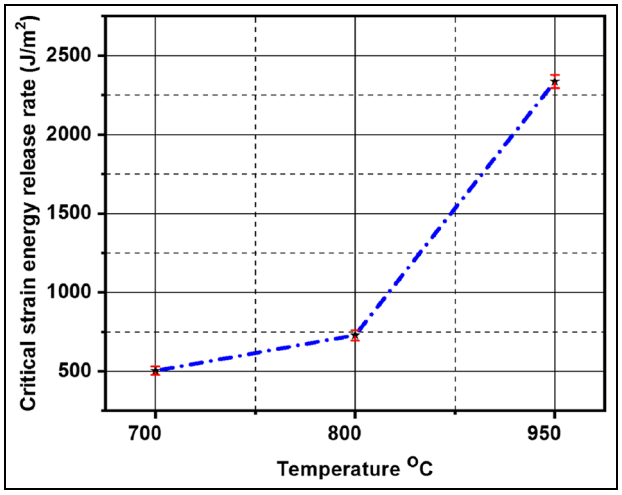

Figure 16. Variation of CSERR versus temperature for mode 2.

hence raising the bond strength. Figure 18(a)–(c) presents the interface micrographs of the bonded sheets fabricated in this study. As observable, the laminates formed at 950°C temperature show better bonding than those formed at lower temperatures (i.e. 800°C and 700°C). These observations are in accordance with the literature and agree with the bond strength results found herein study.

Formability and modes of failure in SPIF of layered sheet

The failure modes for bilayer sheets processed by SPIF can be (i) fracture of one layer only, (ii) fracture of both layers, and (iii) delamination of two sheets. The failure occurring in St-St bilayer sheet at various pre-rolling temperatures is portrayed in Figure 19. It can be seen that the bulk failure occurs for St-St bilayer sheet prepared at different pre-rolling temperatures and the mode that exists is the fracture of both layers. Delamination does not occur in the entire range of formability tests. However, as shown in Figure 20(b) and (c) formability forms a consistent relation with interfacial parameters thereby indicating that fracture formability and delamination formability (if occur) would be directly correlated. Table 1 shows the formability comparison in terms of the maximum wall angle for St-St bilayer sheet. The results depict that the formability of St-St bilayer sheet increases with the enhancement in pre-rolling temperature. This is because the percent tensile area reduction ($\%A_r$) increases with an increase in pre-rolling temperature from 700°C to 950°C. The relationship between $\%A_r$ and formability is shown in Figure 20 revealing that formability increases with an increase in $\%A_r$. Moreover, the St-St bilayer sheet prepared at a pre-rolling temperature of 700°C delaminates without forming into the desired

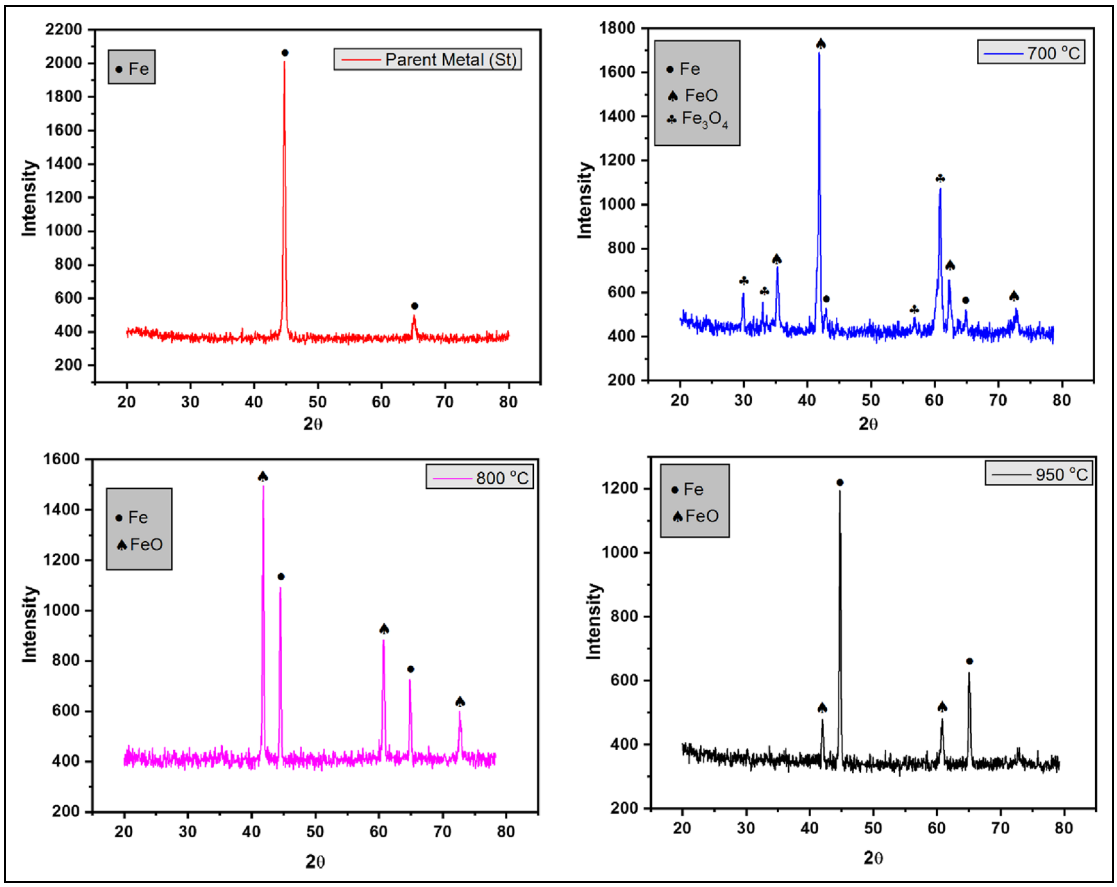

Figure 17. XRD analysis for St-St bilayer sheet at different pre-rolling temperatures.

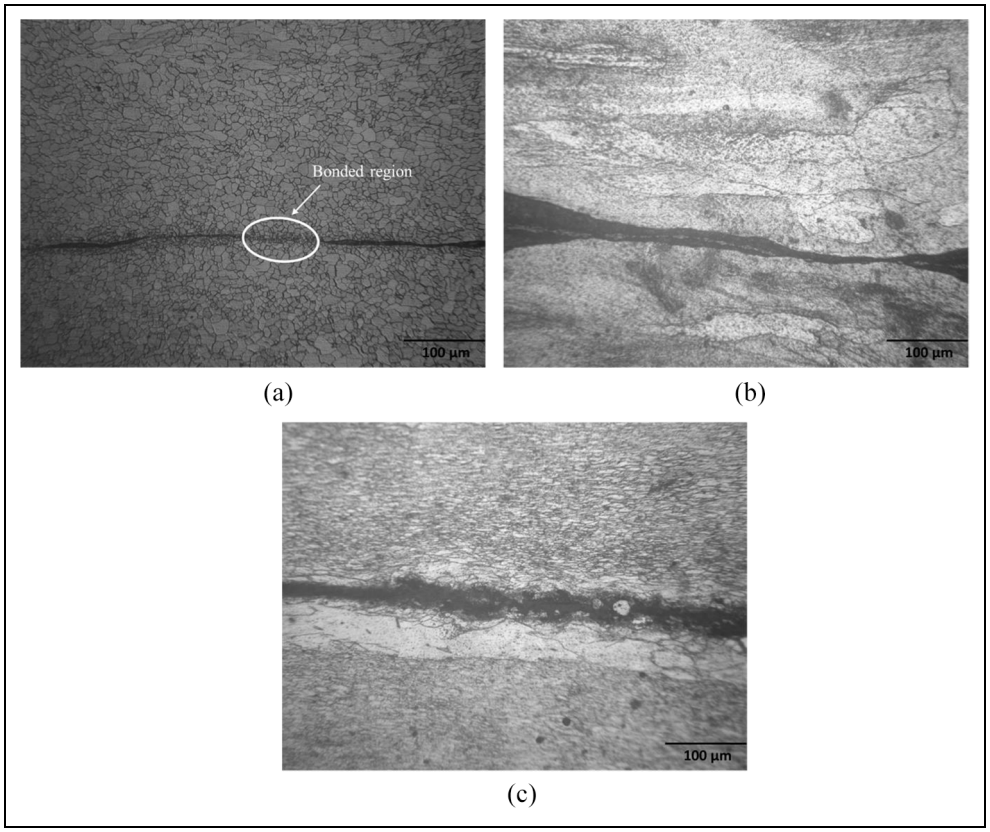

Figure 18. Micrograph of St-St bilayer sheet at (a) 950°C, (b) 800°C, and (c) 700°C.

Table 1. Formability comparison of St-St bilayer sheet for various pre-rolling temperatures.

Forming conditions	Formability (ψ_{max})	% Area reduction
58% TR at pre-rolling temperature 950°C	52.7°	45
58% TR at pre-rolling temperature 800°C	47.8°	39
58% TR at pre-rolling temperature 700°C	Sheets delaminate at the initial tool contact	13

TR: Thickness reduction; ψ_{max}: Maximum wall angle.

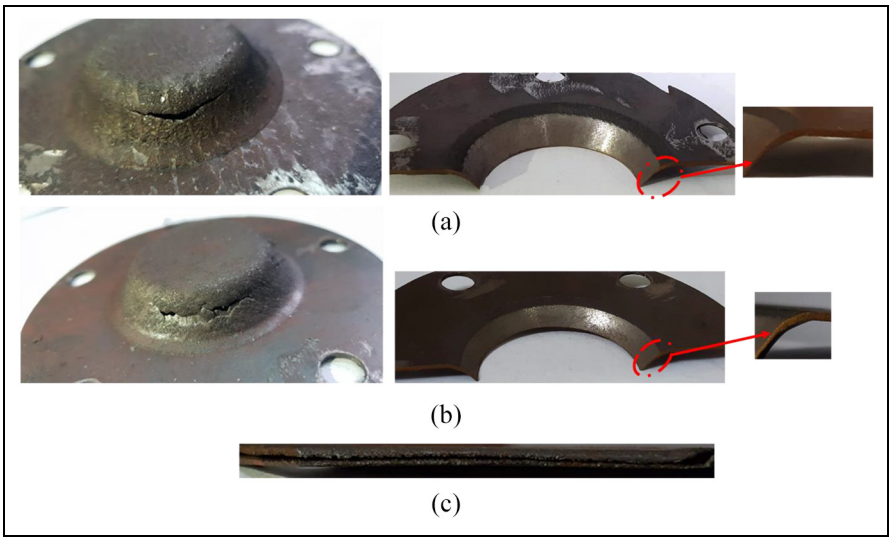

Figure 19. St-St bilayer sheet fracture pattern in SPIF at various conditions: (a) pre-rolling temperature of 950°C, (b) pre-rolling temperature of 800°C, and (c) pre-rolling temperature of 700°C.

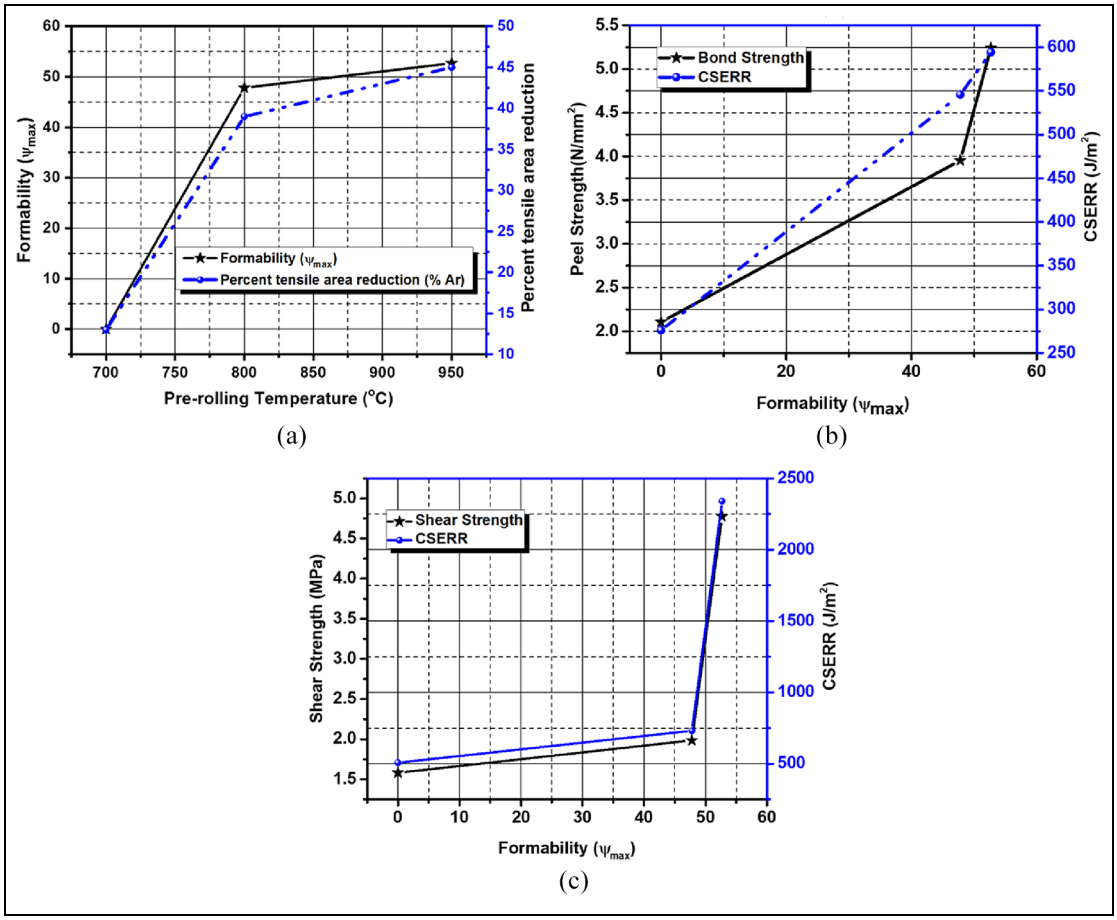

Figure 20. (a) Relationship between area reduction and formability at various pre-rolling temperatures, (b) formability relationship with peel strength and CSERR for mode 1, and (c) formability relationship with shear strength and CSERR for mode 2.

shape when the tool touches the sheet at the start. Thus, for the bilayer sheet to be deformed, the sheet must be heated above the critical temperature.

Conclusion

Following findings can be concluded from this study:

1. The bond strength and CSERR increases with an increase in pre-rolling temperature in both mode 1 and mode 2. The increase in bond strength with an increase in pre-rolling temperature from 700°C to 950°C is 149.5% and 203% in modes 1 and 2, respectively. Whereas, the percentage increase in CSERR is 115% in mode 1 and 367% in mode 2.
2. An increasing trend in formability is observed with an increase in pre-rolling temperature. This is because the $\%A_r$ increases with the increase of pre-rolling temperature. Furthermore, for the St-St bilayer sheet, it is necessary to heat the sheet above the critical temperature to successively deform the sheet into the desired shape.
3. The mode of failure that occurs for St-St bilayer sheet is bulk material failure of both the layers. Thus, it can be concluded that St-St bilayer sheet fails in the same manner as that of the counterpart monolithic sheet. Moreover, formability forms a consistent relation with interfacial parameters.
4. The yield strength of St-St bilayer sheet decreases with an increase in pre-rolling temperature. This can be due to grain hardening and dislocations strengthening at low pre-rolling temperature similar to the phenomenon that occurs in the monolithic sheet.

Declaration of conflicting interests

The author(s) declared no potential conflicts of interest with respect to the research, authorship, and/or publication of this article.

Funding

The author(s) received no financial support for the research, authorship, and/or publication of this article.

ORCID iDs

Ghulam Hussain https://orcid.org/0000-0002-9642-0303
Aaqib Ali https://orcid.org/0000-0002-5661-412X

Muhammad Ilyas https://orcid.org/0000-0002-0496-4195
Wasim A Khan https://orcid.org/0000-0003-1130-7262

References

1. Hagan E and Jeswiet J. A review of conventional and modern single-point sheet metal forming methods. *Proc IMechE, Part B: J Engineering Manufacture* 2003; 217: 213–225.
2. Josue da Silva P and Alvares AJ. Investigation of tool wear in single point incremental sheet forming. *Proc IMechE, Part B: J Engineering Manufacture* 2020; 234: 170–188.
3. Young D and Jeswiet J. Wall thickness variations in single-point incremental forming. *Proc IMechE, Part B: J Engineering Manufacture* 2004; 218: 1453–1459.
4. Siddiqi MUR, Corney JR, Sivaswamy G, et al. Design and validation of a fixture for positive incremental sheet forming. *Proc IMechE, Part B: J Engineering Manufacture* 2018; 232: 629–643.
5. Kurra S, Nasih HR, Regalla S, et al. Parametric study and multi-objective optimization in single-point incremental forming of extra deep drawing steel sheets. *Proc IMechE, Part B: J Engineering Manufacture* 2016; 230: 825–837.
6. Benedetti M, Fontanari V, Monelli B, et al. Single-point incremental forming of sheet metals: experimental study and numerical simulation. *Proc IMechE, Part B: J Engineering Manufacture* 2017; 231: 301–312.
7. Zhang H, Lu B, Chen J, et al. Thickness control in a new flexible hybrid incremental sheet forming process. *Proc IMechE, Part B: J Engineering Manufacture* 2017; 231: 779–791.
8. Ambrogio G, De Napoli L, Filice L, et al. Application of incremental forming process for high customised medical product manufacturing. *J Mater Process Technol* 2005; 162: 156–162.
9. Oleksik V, Pascu A, Deac C, et al. The influence of geometrical parameters on the incremental forming process for knee implants analyzed by numerical simulation. *AIP Conf Proc* 2010; 1252: 1208–1215.
10. Bagudanch I, Lozano-Sánchez LM, Puigpinós L, et al. Manufacturing of polymeric biocompatible cranial geometry by single point incremental forming. *Procedia Eng* 2015; 132: 267–273.
11. Behera AK, Lauwers B and Duflou JR. Tool path generation framework for accurate manufacture of complex 3D sheet metal parts using single point incremental forming. *Comput Ind* 2014; 65: 563–584.
12. Li J, Shen J and Wang B. A multipass incremental sheet forming strategy of a car taillight bracket. *Int J Adv Manuf Technol* 2013; 69: 2229–2236.
13. Basak S, Prasad KS, Mehto A, et al. Parameter optimization and texture evolution in single point incremental sheet forming process. *Proc IMechE, Part B: J Engineering Manufacture* 2020; 234: 126–139.
14. Dhib Z, Guermazi N, Gaspérini M, et al. Cladding of low-carbon steel to austenitic stainless steel by hot-roll bonding: microstructure and mechanical properties before and after welding. *Mater Sci Eng A* 2016; 656: 130–141.
15. Smith L. Engineering with clad steel. *Nickel Dev Inst*. Technical Series No. 10064, 1992.
16. Zhang XP, Yang TH, Castagne S, et al. Proposal of bond criterion for hot roll bonding and its application. *Mater Des* 2011; 32: 2239–2245.
17. Liu BX, Yin FX, Dai XL, et al. The tensile behaviors and fracture characteristics of stainless steel clad plates with different interfacial status. *Mater Sci Eng A* 2017; 679: 172–182.
18. Dhib Z, Guermazi N, Ktari A, et al. Mechanical bonding properties and interfacial morphologies of austenitic stainless steel clad plates. *Mater Sci Eng A* 2017; 696: 374–386.
19. Saboktakin M, Razavi GR and Monajati H. The investigate metallurgical properties of roll bonding titanium clad steel. *Int J Appl Phys Math* 2011; 1: 177.
20. Peng XK, Wuhrer R, Heness G, et al. Effect of rolling temperature on interface and bond strength development of roll bonded copper/aluminium metal laminates. *J Mater Sci* 1999; 34: 2029–2038.
21. Hosseini M and Danesh Manesh H. Bond strength optimization of Ti/Cu/Ti clad composites produced by roll-bonding. *Mater Des* 2015; 81: 122–132.
22. Al-Ghamdi KA and Hussain G. SPIF of Cu/Steel clad sheet: annealing effect on bond force and formability. *Mater Manuf Process* 2016; 31: 758–763.
23. Al-Ghamdi KA and Hussain G. Parameter-formability relationship in ISF of tri-layered Cu-Steel-Cu composite sheet metal: response surface and microscopic analyses. *Int J Precis Eng Manuf* 2016; 17: 1633–1642.
24. Al-Ghamdi KA and Hussain G. On the comparison of formability of roll-bonded steel-Cu composite sheet metal in incremental forming and stamping processes. *Int J Adv Manuf Technol* 2016; 87: 267–278.
25. Alinaghian M, Alinaghian I and Honarpisheh M. Residual stress measurement of single point incremental formed Al/Cu bimetal using incremental hole-drilling method. *Int J Light Mater Manuf* 2019; 2: 131–139.
26. Gheysarian A and Honarpisheh M. An experimental study on the process parameters of incremental forming of explosively-welded Al/Cu bimetal. *J Comput Appl Res Mech Eng* 2017; 7: 73–83.
27. Honarpisheh M, Mohammadi Jobedar M and Alinaghian I. Multi-response optimization on single-point incremental forming of hyperbolic shape Al-1050/Cu bimetal using response surface methodology. *Int J Adv Manuf Technol* 2018; 96: 3069–3080.
28. Ashouri R and Shahrajabian H. Experimental investigation of incremental forming process of bilayer hybrid brass/St13 sheets. *ADMT J* 2017; 10: 127–135.
29. Hassan M, Hussain G, Ilyas M, et al. Delamination analysis in single – point incremental forming of steel / steel bi – layer sheet metal. *Arch Civ Mech Eng* 2020; 1: 1–14.
30. ASTM Int. Standard test methods for tension testing of metallic materials 1. *ASTM* 2009; C: 1–27.
31. Resistance P. Peel resistance of adhesives (T-Peel test)'. *Current* 2001; 2: 3–5.
32. Hassan M, Ali A, Ilyas M, et al. Experimental and numerical simulation of steel/steel (St/St) interface in bi-layer sheet metal. *Int J Light Mater Manuf* 2019; 2: 89–96.
33. Roylance D. *Introduction to fracture mechanics*. Cambridge: Department of Materials Science and Engineering, Massachusetts Institute of Technology, 2001, pp.1–17

34. ASTM D 1002. Standard test method for apparent shear strength of single-lap-joint adhesively bonded metal specimens by tension loading (metal-to-metal). *Standards* 2005; 1: 1–5.
35. Tang C, Liu Z, Zhou D, et al. Surface treatment with the cold roll bonding process for an aluminum alloy and mild ssteel. *Strength Mater* 2015; 47: 150–155.
36. Noorman DC. *Cohesive zone modelling in adhesively bonded joints: analysis on crack propagation in adhesives and adherends*. Delft: Delft University of Technology, 2014.
37. Allwood JM, Bramley AN, Ridgman TW, et al. A novel method for the rapid production of inexpensive dies and moulds with surfaces made by incremental sheet forming. *Proc IMechE, Part B: J Engineering Manufacture* 2006; 220: 323–327.
38. Hussain G and Gao L. A novel method to test the thinning limits of sheet metals in negative incremental forming. *Int J Mach Tools Manuf* 2007; 47: 419–435.
39. Jeswiet J and Young D. Forming limit diagrams for single-point incremental forming of aluminium sheet. *Proc IMechE, Part B: J Engineering Manufacture* 2005; 219: 359–364.
40. Guo B, Fan L, Wang Q, et al. Effect of finish rolling temperature on the microstructure and tensile properties of Nb–Ti Microalloyed X90 pipeline steel. *Metals (Basel)* 2016; 6: 323.
41. Li Z and Wu D. Influence of hot rolling conditions on the mechanical properties of hot rolled TRIP steel. *J Wuhan Univ Technol Sci Ed* 2008; 23: 74–79.
42. Yan H and Lenard JG. A study of warm and cold roll-bonding of an aluminium alloy. *Mater Sci Eng A* 2004; 385: 419–428.
43. Abbasi M and Toroghinejad MR. Effects of processing parameters on the bond strength of Cu/Cu roll-bonded strips. *J Mater Process Technol* 2010; 210: 560–563.
44. Eizadjou M, Danesh Manesh H and Janghorban K. Investigation of roll bonding between aluminum alloy strips. *Mater Des* 2008; 29: 909–913.